CHEMICAL ENGINEERING TRANSACTIONS
VOL. 100, 2023
A publication of AIDIC
The Italian Association of Chemical Engineering
Online at www.cetjournal.it
Guest Editors: Sauro Pierucci, Flavio Manenti
Copyright © 2023, AIDIC Servizi S.r.l.
ISBN 979-12-81206-03-8; **ISSN** 2283-9216
DOI: 10.3303/CET23100048

Dynamic Simulation of Breakthrough Curves on Multilayered Beds for Hydrogen Purification from Syngas Mixtures

Federico Cecchini[a]*, Valentina Innocenzi[a], Valerio M. Corradetti[b], Marina Prisciandaro[a]

[a]University of L'Aquila, Department of Industrial and Information Engineering and Economics (DIIIE), Piazzale E.Pontieri 1-loc. Monteluco di Roio 67100 L'Aquila Italy
[b]ENERECO S.p.A., Via D. Carpazi 14, 61032 Fano (PU) - Italy
federico.cecchini@graduate.univaq.it

This paper modeled the behavior of a double-layer adsorption column to process a current with a Syngas-like composition. The modeling was performed on Aspen Adsorption software to evaluate its performance by comparison with experimental data found in the literature. The simulation aims is to evaluate the modeled system for potential use in PSA systems for hydrogen purification from a Syngas stream, with successive simulations on different plant scales.

1. Introduction

Pressure Swing Adsorption (PSA) is an excellent gas mixture separation and purification method. Currently, PSA technologies are used for hydrogen purification in more than 85% of global hydrogen production systems (Tao et al., 2019).
PSA systems have grown in popularity over the last few decades, owing to their ease of use and low operating costs. These systems' main applications are the recovery of high-purity hydrogen, methane, and carbon dioxide and the recovery of nitrogen and oxygen (Linde Engineering).
One of the primary benefits of using PSA systems is their extreme simplicity, which results in process reliability with relatively low investment and maintenance costs. Furthermore, these systems do not require many resources, making them suitable for various applications. Because the gas purification technology is dry, it does not require water and thus does not cause aqueous effluent problems. Moreover, no heat is needed for the process. As a result, operating costs are low, with energy costs limited to the need for pressurized gas (Bauer et al., 2013).
The flexibility of PSA cycles has been studied in the context of energy savings and in areas other than hydrogen production (Šulc et al., 2021).
Currently, no hydrogen-selective adsorbents are available (Liemberger et al., 2017). The use of multiple adsorbents in adsorption beds as layers is an important modality for current gas purification technologies.
In the design of a PSA system, the logic is to have each species adsorbed onto the specific solid to achieve an adequate trade-off between favorable adsorption and easy desorption.
Instead of using multiple layers, a series of columns with different adsorbent beds could be used to create an adsorption gradient (Chlendi et al., 1995).
These performance enhancements can also be pursued by developing better-performing adsorbents and changing PSA system operating schemes and varying process parameters (Ribeiro et al., 2008).
In chemical process design, complex mathematical models are frequently used to calculate process streams' chemical and physical properties. The use of specific simulation software provides a significant advantage for analyzing existing processes, designing new processes, implementing control strategies, and comparing different processes to determine the best solution as needed (Cimini et al., 2005).
The Aspen Adsorption software was used in this study to replicate experimental results found in the literature for potential use in PSA systems for hydrogen purification from a Syngas stream.

Paper Received: 10 December 2022; Revised: 27 April 2023; Accepted: 14 May 2023
Please cite this article as: Cecchini F., Innocenzi V., Corradetti V.M., Prisciandaro M., 2023, Dynamic Simulation of Breakthrough Curves on Multilayered Beds for Hydrogen Purification from Syngas Mixtures, Chemical Engineering Transactions, 100, 283-288 DOI:10.3303/CET23100048

2. Model description

Aspen Adsorption is a comprehensive simulator for adsorption process analysis, design, simulation, and optimization. For example, this software can simulate ion exchange, liquid phase adsorption, and gas phase adsorption processes. The Gas Cyclic Steady State (gCSS) calculation mode is also presented to simulate cyclic processes such as PSA. The simulator supports the use of Aspen Properties components' physical and thermodynamic properties; there is also a wide range of material and energy transport models. For the simulation of complex processes such as adsorption, finite element solvers such as Comsol Multiphysics (Xiao et al. 2016) or Fortran-based packages such as ODEPACK (Chou et al. 2013) are frequently used. Process simulators such as gPROMS (Ribeiro et al. 2008) or Aspen Adsorption (Zhang et al. 2021) are used less frequently. The literature mostly reports on cases where these software were used to optimize 2-bed PSA or VPSA processes. Cases of simulation of breakthrough curves on dedicated software, such as Aspen Adsorption, are more uncommon. As a result, Aspen Adsorption was chosen for the mathematical implementation of the models described, mostly because it can interact with all AspenTech packages.

For the characteristics of the adsorbent materials and the experimental system to be simulated, the modeling work refers to the article by Jee and coworkers (Jee et al., 2001). The characteristics of the adsorbents and the adsorption bed are summarized in Table 1.

Table 2 displays the simulation's input stream characteristics and working data.

The Peng Robinson equation of state was chosen for the gas mixture under consideration. Aspen Properties calculates the majority of gas phase properties using these equations of state.

For the material balance assumption, Eq. (1), the dispersion term is removed from the material balance, resulting in plug flow with a zero dispersion coefficient (infinite Peclet number). The axial dispersion term can be ignored to simplify the mathematical model, as demonstrated in other studies (Xiao et al. 2016).

$$\frac{\partial C_i}{\partial t} + \frac{(1-\epsilon_t)}{\epsilon_t}\frac{\partial q_i}{\partial t} + u_z \frac{\partial C_i}{\partial z} = D_L \frac{\partial^2 C_i}{\partial z^2} = 0 \tag{1}$$

Table 1 Characteristics of Adsorbents and Adsorption Beds (Jee et al. 2001; Xiao et al. 2016).

Adsorbent	Activated carbon	Zeolite 5A
Type	Granular	Sphere
Average pellet size, $R_p(mm)$	1.15	1.57
Pellet density, $\rho_p \left(\frac{g}{cm^3}\right)$	0.85	1.16
Heat capacity, $C_{ps} \left(\frac{cal}{gK}\right)$	0.25	0.22
Inter-particle voidage, $\epsilon_i(-)$	0.433	0.357
Total void porosity, $\epsilon_t(-)$	0.78	0.77
Bed density, $\rho_B \left(\frac{g}{cm^3}\right)$	0.482	0.746
Thermal conductivity, $k_s \left(\frac{W}{m\,K}\right)$	0.406	0.462
Adsorption bed		
Length, L (cm)	100	
Inside radius, $R_{Bi}(cm)$	1.855	
Outside radius, $R_{Bo}(cm)$	2.123	
Heat capacity of column, $C_{pw} \left(\frac{cal}{gK}\right)$	0.120	
Wall thermal conductivity, $k_W \left(\frac{W}{m\,K}\right)$	45	
Density of column, $\rho_w \left(\frac{g}{cm^3}\right)$	7.830	
Internal heat transfer coefficient, $h_i \left(\frac{cal}{cm^2 Ks}\right)$	9.2 x 10^{-4}	
External heat transfer coefficient, $h_o \left(\frac{cal}{cm^2 Ks}\right)$	3.4 x 10^{-4}	

The temperature of the process is greatly influenced by the adsorption process. The temperature, in turn, affects the entire adsorption process. The general form of energy balance is described in Eq. (2):

$$-k_g\epsilon_i \frac{\partial^2 T_g}{\partial z^2} + C_{vg}u_z\rho_g\frac{\partial T}{\partial z} + \epsilon_b C_{vg}\rho_g\frac{\partial T_g}{\partial t} + P\frac{\partial u_g}{\partial z} + h_i a_p\left(T_g - T_s\right) + \frac{4h_i}{D_B}\left(T_g - T_W\right) \tag{2}$$

Table 2: characteristics and composition of the process stream.

Gas flow rate, F $\left(\frac{LSTP}{min}\right)$	8.6
Feed Temperature, T (K)	298.15
Gas thermal conductivity, $k_s\left(\frac{W}{m\,K}\right)$	0.084
Adsorption pressure, P (atm)	10

Gas Mixture	% vol.
H_2	56.4
CH_4	26.6
CO	8.4
N_2	5.5
CO_2	3.1

The heat transfer to the environment, Eq. (3), was considered rigorous, with the following energy balances:

$$-k_W\frac{\partial^2 T_W}{\partial z^2}+\rho_W C_{pw}\frac{\partial T_w}{\partial t}-h_i\frac{4D_B}{(D_B+W_T)^2-D_B^2}\left(T_g-T_W\right)+h_o\frac{4(D_B+W_T)^2}{(D_B+W_T)^2-D_B^2}(T_W-T_{amb})=0 \quad (3)$$

Since it was assumed that the adsorption was non-isothermal, the temperature of the adsorbent is defined as reported in Eq. (4) (Wood et al., 2018):

$$\rho_s C_{ps}\frac{\partial T_s}{\partial t}+\rho_s\sum_i^n Q_i\frac{\partial q_i}{\partial t}+h_i a_p\left(T_g-T_s\right)=0 \quad (4)$$

For momentum balance, the Ergun equation was chosen, Eq. (5), which combines the descriptions of pressure drops by the Karman-Kozeny equation for laminar flow and the Burke-Plummer equation for turbulent flow.

$$\frac{\partial P}{\partial z}=-\left(\frac{1.5x10^{-3}\mu_g(1-\epsilon_i)^2}{\left(2r_p\psi\right)^2\epsilon_i^3}+1.75x10^{-5}M_w\rho_g\frac{(1-\epsilon_i)}{2r_p\psi\epsilon_i^3}u_z^2\right) \quad (5)$$

The linear driving force (LDF) model with a single lumped mass transfer parameter, Eq. (6), describes the sorption rate into the adsorbent.

$$\frac{\partial q_i}{\partial t}=\omega_i\,(q_i^*-q_i) \quad (6)$$

According to the literature, the optimal activated carbon/zeolite ratio for the adsorption of the mixture under evaluation is 0.65 (Yang & Lee 1998).

Given the large number of compounds to be removed from the stream, each layer will remove one or more contaminants based on affinity. Generally, an initial alumina or silica gel layer will adsorb moisture in typical syngas or catalytic reforming gas compositions. Then, along with CO_2, a layer of activated carbon will adsorb methane and any heavy hydrocarbons. On the other hand, the final layer will be zeolite, due to its superior CO and N_2 adsorption capabilities. CO_2 and H_2O are strongly adsorbed onto zeolite, making desorption difficult. As the work cycles progress, these components accumulate in the zeolite (Ribeiro et al., 2008).

The Extended Langmuir-Freundlich experimental isotherm, Eq.(7), predicted multicomponent adsorption equilibrium:

$$q_i=\frac{q_{mi}B_iP_i^{ni}}{1+\sum_{j=1}^n B_jP_j^{nj}} \quad (7)$$

Where: $q_m=k_1+k_2T$, $B=k_3\,exp\frac{k_4}{T}$ e $n_i=k_5+\frac{k_6}{T}$.

Table 3 summarizes the isotherm parameters and the LDF coefficients (Jee et al., 2001).

Because the isotherm used in the simulations is not available in the Gas Dynamic simulation model, it was created using the Aspen Custom Modeler code.

3. Results

The described model simulates the behavior of a laboratory-scale adsorption column using data taken from the literature. The simulation input data concern the input stream's composition, flow rate, temperature, and pressure. The outputs compared to experimental data reported by Jee and coworkers (Jee et al., 2001) concern breakthrough curves, concentration trends, and temperature trends in the bed.

Table 3: Extended Langmuir-Freundlich Parameters and LDF Coefficient for Activated Carbon and Zeolite 5A (Zhang et al. 2021).

	k_1	$k_2 x 10^2$	$k_3 x 10^4$	k_4	k_5	k_6	$LDF\ coeff.$ ω_i	Q
	$\left(\frac{mmol}{g}\right)$	$\left(\frac{mmol}{gK}\right)$	$\left(\frac{1}{atm}\right)$	(K)	$(-)$	(K)	$\left(\frac{1}{s}\right)$	$\left(\frac{cal}{mol}\right)$
Activated carbon								
H_2	16.943	-2.100	0.625	1229	0.980	43.03	0.700	2880
CH_4	23.860	-5.621	34.780	1159	1.618	-248.9	0.195	4290
CO	33.850	-9.072	2.311	1751	3.053	-654.4	0.150	4300
N_2	1.644	-0.073	545.0	326	0.908	0.991	0.261	1660
CO_2	28.797	-7.000	100.0	1030	0.999	-37.04	0.036	5240
Zeolite 5A								
H_2	4.314	-1.060	25.15	458	0.986	43.03	0.700	2800
CH_4	5.833	-1.192	6.507	1731	0.820	53.15	0.147	5400
CO	11.845	-3.130	202.0	763	3.823	-931.3	0.063	5300
N_2	4.813	-0.668	5.695	1531	0.842	-7.467	0.099	5470
CO_2	10.030	-1.858	1.578	207	-5.648	2098.0	0.014	9330

The flowsheet used in the adsorption column simulation is shown in Figure 1.

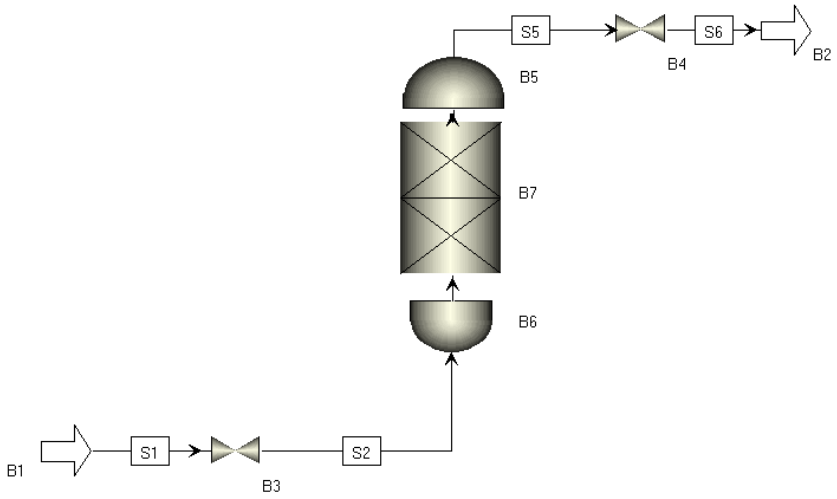

Figure 1: simulation flowsheet.

Figure 2 shows the breakthrough curves for the gas mixture in the bed. N_2 is the first component to pass through the bed, followed by CO and CH_4. CO_2 is the last component to pass through the bed. Several roll-ups can be seen here, which go to distort the H_2 curve, confirming the phenomenon observed experimentally. It is also noted that the obtained results are comparable to the experimental results.

Figure 3 (a) shows the profiles of component concentrations in the bed mixture of 100 cm length after 180 seconds of simulation, while Figure 3 (b) shows the same profiles after 300 seconds. The simulation results match the experimental results in terms of trends. The concentration plot for t=300 s confirms the upstream reports by showing concentration peaks for CO and N_2 in the zeolite section of the bed, while CH_4 and CO_2 are adsorbed by activated carbon in the first layer of the bed.Figure 3 (c) illustrates the temperature profiles in the bed, 180 and 300 seconds after the simulation began, respectively. The experimental data confirm the presence

of a second peak in the temperature profile at 180 s in the bed layer responsible for N_2 and CO adsorption. It has also been observed that the temperature profile tends to become more uniform over time.

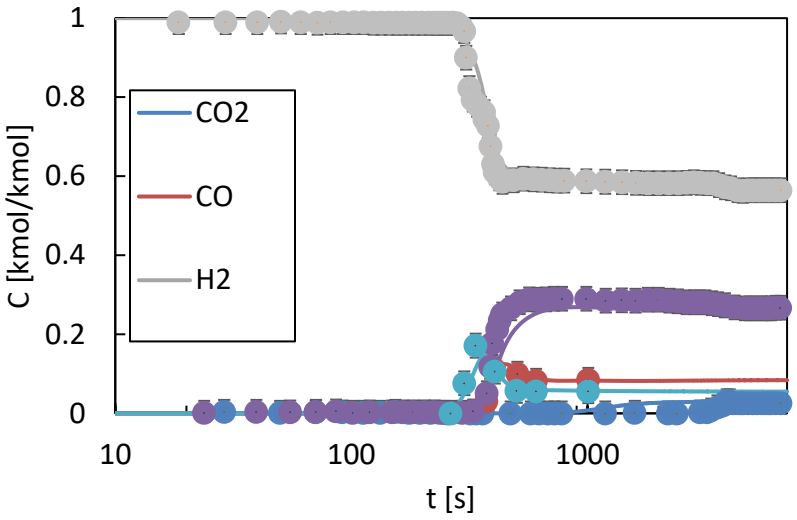

Figure 2: Breakthrough curves for the processed mixture.

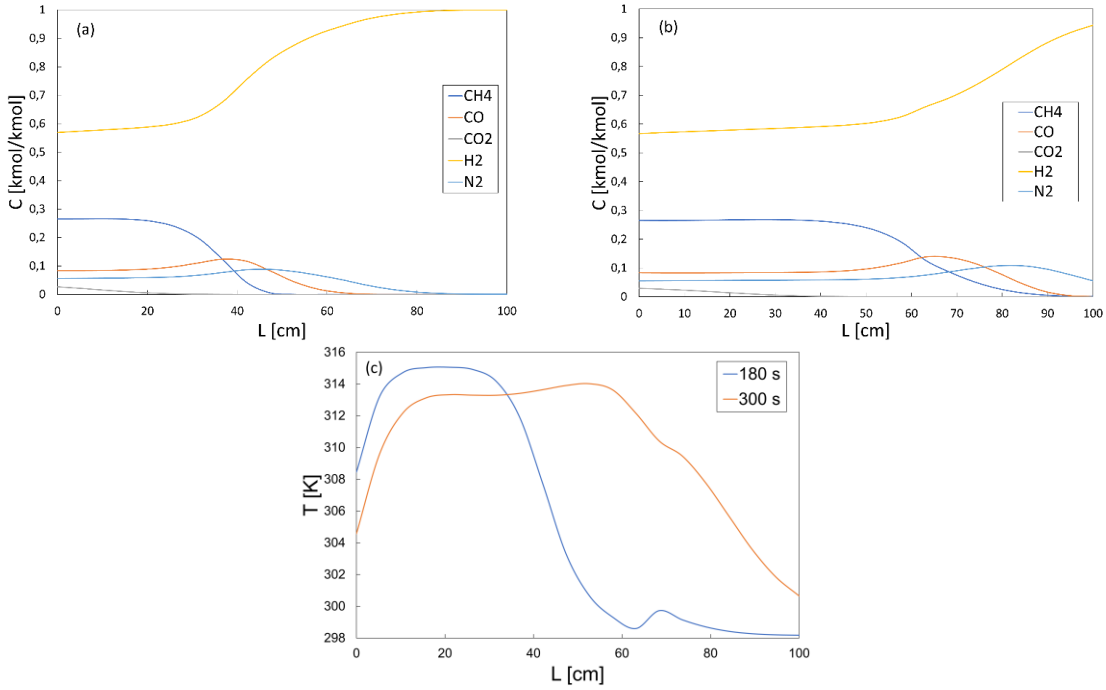

Figure 3: concentration profiles in the bed at t=180 s (a) and t=300 s (b); temperature profiles in the bed at 180 and 300 s (c).

4. Conclusions

In this paper, Aspen Adsorption software was used to simulate the behavior of breakthrough curves, concentration, and temperature profiles within an adsorption bed. The results, which were confirmed by experimental data, show how the mathematical models already included in the software can be used to predict the behavior of experimental adsorption systems. The program's adaptability was also tested by including an isotherm not found in the library of Aspen Adsorption's dynamic gas simulation mode. Future work will involve the simulation of multibed PSA systems, first on a laboratory scale and then progressing to semi-industrial scale simulation.

Nomenclature

L – bed length, m
L_c – fin length, m
k_i – isotherm parameters, -
P – pressure, atm
P_i – partial pressure, atm
T – temperature, K
T_g – gas temperature, K
T_s – solid temperature, K
T_w – wall temperature, K
q_i – amount adsorbed, mol/g
q_{mi} – equilibrium parameter for the Langmuir Freundlich model, mol/g
C_i – molar concentration in the gas phase, kmol/kmol
C_{vg} – Specific gas-phase heat capacity, cal/(mol K)
z – axial distance trough column, m
u_z – superficial velocity of gas flow, m/s
D_L – axial dispersion coefficient, m^2/s
ρ_g – gas density, g/cm^3
D_B – bed diameter, m
W_T – wall thickness, m
ψ – spherical factor, -
a_p – surface area per volume unit, 1/m
μ_g – gas mixture viscosity, cP
M_w – Molecular weight of the gaseous mixture, kg/kmol

References

Bauer F., Hulteberg C., Persson T., Tamm D., 2013. Biogas upgrading-Review of commercial technologies (Biogasuppgradering-Granskning av kommersiella tekniker) SGC Rapport 2013:270 'Catalyzing energygas development for sustainable solutions'.

Chlendi M., Tondeur D., 1995. Dynamic behaviour of layered columns in pressure swing adsorption, vol. 9.

Chou C.T., Chen F.H., Huang Y.J., Yang H.S., 2013. Carbon Dioxide Capture and Hydrogen Purification from Synthesis Gas by Pressure Swing Adsorption, Chemical Engineering Transactions, 32, 1855–1860.

Cimini S., Prisciandaro M., Barba D., 2005. Simulation of a waste incineration process with flue-gas cleaning and heat recovery sections using Aspen Plus, Waste Management, 25(2), 171–175.

Jee J.G., Kim M.B., Lee C.H., 2001. Adsorption characteristics of hydrogen mixtures in a layered bed: Binary, ternary, and five-component mixtures, Industrial and Engineering Chemistry Research, 40(3), 868–878.

Liemberger W., Groß M., Miltner M., Harasek M., 2017. Experimental analysis of membrane and pressure swing adsorption (PSA) for the hydrogen separation from natural gas, Journal of Cleaner Production, 167, 896–907.

Linde Engineering, no date, Hydrogen Recovery by Pressure Swing Adsorption.

Ribeiro A.M., Grande C.A., Lopes F.V.S., Loureiro J.M., Rodrigues A.E., 2008. A parametric study of layered bed PSA for hydrogen purification, Chemical Engineering Science, 63(21), 5258–5273.

Šulc R., Ditl, P., 2021. The Potential of Energy Savings in Oxygen Production by Pressure Swing Adsorption, Chemical Engineering Transactions, 86, 313–318.

Tao W., Ma S., Xiao J., Bénard P., Chahine R., 2019. Simulation and optimization for hydrogen purification performance of vacuum pressure swing adsorption, Energy Procedia, vol. 158, 1917–1923, Elsevier Ltd.

Wood K.R., Yih A.L., Yueying Y., 2018. Design, simulation and optimization of adsorptive and chromatographic separations: A hands-on approach.

Xiao J., Peng Y., Bénard P., Chahine R., 2016. Thermal effects on breakthrough curves of pressure swing adsorption for hydrogen purification, International Journal of Hydrogen Energy, 41(19), 8236–8245.

Yang J., Lee C.H., 1998. Adsorption dynamics of a layered bed PSA for H2 recovery from coke oven gas, AIChE Journal, 44(6), 1325–1334.

Zhang N., Bénard P., Chahine R., Yang T., Xiao J., 2021. Optimization of pressure swing adsorption for hydrogen purification based on Box-Behnken design method, International Journal of Hydrogen Energy, 46(7), 5403–5417.